ISSN 1674-1056
http://cpb.iphy.ac.cn
http://iopscience.iop.org/cpb
中国物理 B
Chinese Physics
中国物理 Chinese Physics B

Ion track-based nanowire arrays with gradient and programmable diameters towards rational light management

Ran Huang(黄冉), Jiaming Zhang(张家明), Fangfang Xu(徐芳芳), Jie Liu(刘杰), Huijun Yao(姚会军), Yonghui Chen(陈永辉), and Jinglai Duan(段敬来)

Citation: Chin. Phys. B, 2021, 30 (**8**): 086105. DOI: 10.1088/1674-1056/ac078a
Journal homepage: http://cpb.iphy.ac.cn; http://iopscience.iop.org/cpb

What follows is a list of articles you may be interested in

Mechanical property and deformation mechanism of gold nanowire with non-uniform distribution of twinned boundaries: A molecular dynamics simulation study

Qi-Xin Xiao(肖启鑫), Zhao-Yang Hou(侯兆阳), Chang Li(李昌), and Yuan Niu(牛媛)
Chin. Phys. B, 2021, 30 (**5**): 056101. DOI: 10.1088/1674-1056/abd162

Exciton emissions of CdS nanowire array fabricated on Cd foil by the solvothermal method

Yong Li(李勇), Peng-Fei Ji(姬鹏飞), Ya-Juan Hao(郝亚娟), Yue-Li Song(宋月丽), Feng-Qun Zhou(周丰群), and Shu-Qing Yuan(袁书卿)
Chin. Phys. B, 2021, 30 (**1**): 016104. DOI: 10.1088/1674-1056/abbbf1

Structural and electronic properties of transition-metal chalcogenides Mo_5S_4 nanowires

Ming-Shuai Qiu(邱明帅), Huai-Hong Guo(郭怀红), Ye Zhang(张也), Bao-Juan Dong(董宝娟), Sajjad Ali(阿里.萨贾德), Teng Yang(杨腾)
Chin. Phys. B, 2019, 28 (**10**): 106103. DOI: 10.1088/1674-1056/ab3f9a

Light trapping and optical absorption enhancement in vertical semiconductor Si/SiO_2 nanowire arrays

Ying Wang(王莹), Xin-Hua Li(李新化)
Chin. Phys. B, 2018, 27 (**2**): 026102. DOI: 10.1088/1674-1056/27/2/026102

Synthesis and magnetotransport properties of Bi_2Se_3 nanowires

Kang Zhang(张亢), Haiyang Pan(潘海洋), Zhongxia Wei(魏仲夏), Minhao Zhang(张敏昊), Fengqi Song(宋凤麒), Xuefeng Wang(王学锋), Rong Zhang(张荣)
Chin. Phys. B, 2017, 26 (**9**): 096101. DOI: 10.1088/1674-1056/26/9/096101

SPECIAL TOPIC — Ion beam modification of materials and applications

Ion track-based nanowire arrays with gradient and programmable diameters towards rational light management*

Ran Huang(黄冉)[1,2], Jiaming Zhang(张家明)[1,2], Fangfang Xu(徐芳芳)[1,2], Jie Liu(刘杰)[1,2], Huijun Yao(姚会军)[1,2,3,4], Yonghui Chen(陈永辉)[1,2,3,4], and Jinglai Duan(段敬来)[1,2,3,4,†]

[1] Institute of Modern Physics, Chinese Academy of Sciences, Lanzhou 730000, China
[2] School of Nuclear Science and Technology, University of Chinese Academy of Sciences, Beijing 100049, China
[3] Advanced Energy Science and Technology Guangdong Laboratory, Huizhou 516000, China
[4] Huizhou Research Center of Ion Sciences, Huizhou 516000, China

(Received 1 March 2021; revised manuscript received 23 March 2021; accepted manuscript online 3 June 2021)

Integrating nanowires with nonuniform diameter and random spatial distribution into an array can afford unconventional and additional means for modulating optical response. However, experimental realization of such a nanowire array is quite challenging. In this work, we propose a new fabrication strategy which takes advantage of ion track technology, via sequential swift heavy ion irradiation and ion track etching. Based on this strategy, we unprecedentedly realize nanowire arrays, using gold as an example, with gradient and programmable diameters in a controlled manner. We further demonstrate that such nanowire arrays can support broadband, tunable, and enhanced plasmonic responses. We believe that our new type of nanowire arrays will find great potential in applications such as light management and optoelectronic devices.

Keywords: ion track technology, nanowire, plasmonics, light management

PACS: 61.72.−y, 62.23.Hj, 73.20.Mf, 87.80.Cc **DOI:** 10.1088/1674-1056/ac078a

1. Introduction

Light management copes with the process to manipulate the interplay between photons and materials and devices at micro/nanoscopic scales.[1,2] Extensive studies have proven that light management, though tuning optical reflectance, scattering, transmittance, and absorption, can strikingly improve the performance of optical and photonic devices. Up to date, light management has opened up potential applications in diverse fields including nanomotor/nanorobot,[3,4] optoelectronic devices,[5–10] solar cells,[11,12] chemical/biological sensors,[13,14] photocatalysis,[15,16] and others. One notable example is the demonstration that the nanostructured silicon ultraviolet photodiodes can reach a theoretical limit-breaking external quantum efficiency above 130%, where dramatically enhanced light absorption via nanotexturing plays a significant role for the ultrahigh efficiency improvement.[8] Another paradigmatic application of light management is photocatalysis. A recent report shows that, taking benefit of near unity sunlight harvesting enabled by cobalt plasmonic superstructures, the photothermal hydrogenation of carbon dioxide shows a 20-fold rate increase, as comparing with the conventional silica-supported cobalt catalyst.[17] Among diverse forms of light management, spectral matching, broadband response and tunability, and enhancing light absorption are peculiarly demanded and a wealthy of structures have been developed. Among others, nanowires have attracted a great deal of interest because of their unusual optical properties and potential applications in optoelectronics, plasmonics, and other nanodevices. For instance, tunable spectral responsivity that facilitates the remote control has been realized in light-powered nanowire nanomotors.[18] Bi_2Se_3 nanowires/Si heterostructure photo-detectors exhibited excellent detection performance with an optimized responsivity in a broad spectral range from 380 nm to 1310 nm.[19] It has also been reported recently that, owing to light being guided inside the nanowires (NWs) in the form of the exciton–polariton, nanowires show slow down light and enhance absorption to improve optoelectronic device performance with refractive index increasing sharply both in real and imaginary parts.[20] In photovoltaics, nanowires can exert paramount influence on the light absorption and thus improve the conversion efficiency.[21] On the other hand, besides broadband response, band tunability or enhancing light absorption achieved by changing the materials of nanowires as mentioned in the above report, it can also be achieved by adjusting the structure of nanowires. For instance, band response can be easily modulated by controlling the diameter of nanowires, so as to obtain more efficient photoelectric devices.[4,22,23] For example, a single silicon nanowire can modulate the spectral response to offer more freedom and flexibility of light controlling by changing the nanowire's diameter due to the optical resonance inside the nanowire.[4] In addition, the special nanotree structure composed of a num-

*Project supported by the National Natural Science Foundation of China (Grant Nos. U1932210, 12005270, and 11975114).
†Corresponding author. E-mail: j.duan@impcas.ac.cn
© 2021 Chinese Physical Society and IOP Publishing Ltd

ber of nanowires can easily code with a distinct spectral response in the visible spectrum by loading different dyes.[24] However, a growing demand of optoelectronic devices for light control requires their performance with a broader spectral response range, especially through tuning broad spectral response and enhancing absorption for accurate control. For advancing these applications, nanowires have been rationally engineered to tailor their optical properties so as to realize broadband response and tunability, and enhanced light absorption or antireflection, via elegant designs. Counterintuitively, a series of theoretical works have predicted that arrays of parallel aligned wires with nonuniform diameter would gain broadband spectral response resulting from diameter-modulated optical mode.[21,25–27] More surprisingly, wires in random distribution can even attain enhanced light absorption in comparison to ordered distribution.[25,27,28] In other words, integrating nanowires with nonuniform diameter and random distribution can afford unconventional and additional means for modulating optical response of nanowires. However, experimental implementation of such a nontrivial wire configuration is rare, possibly due to the difficulties of fabrication, in particular for metallic plasmonic wires.

Here, we experimentally demonstrate that such a complex wire configuration can be fashioned by an innovative and straightforward template method based on ion track technology. Optical characterizations show that the band frequencies and width can be delicately modulated. The wires also show enhanced light absorption over the entire absorption band. The mechanism of such an extraordinary optical response is explained and discussed in terms of diameter-dependent and interwire scattering-induced plasmonic resonances. We believe that our creative fabrication strategy initiates a new scenario for fabricating novel nanowire scaffolds and the obtained metallic plasmonic nanowire architectures can find great potential in fundamental plasmonics and practical applications in optoelectronics, enhanced spectroscopies, broadband photodetection, and solar light harvesting.

2. Experiment

Gold nanowire arrays with gradient diameters were fabricated by ion track technology in combination with electrochemical deposition. First, polycarbonate (PC) foils of 30 μm thickness were irradiated by 25 MeV/u ^{86}Kr ions accelerated by the Heavy Ion Research Facility in Lanzhou (HIRFL). The irradiation fluence was 1×10^7 ions/cm^2. After every irradiation, each surface of the foils was illuminated with ultraviolet light (MUA-165, Mejiro Genossen, Japan) for 2 hours. Then, the ion tracks produced by ion irradiation were etched with 5 M NaOH at 50 °C and the etching process transformed ion tracks into nanopores whose diameter is solely controlled by etching time. Taking Fig. 2(a) as an example, after the first, second, and third irradiation, the sample was etched for 5 min, 3 min, and 4 min with 5 M NaOH at 50 °C, respectively. Finally, gold nanowires were deposited into nanopores by electrochemical deposition using potentiostatic direct current (dc) deposition. For electrodeposition of gold wires, a thin layer of gold (∼ 70 nm) was sputtered (Q150TS Plus, Quorum, UK) on one surface of each PC template and reinforced with an electrodeposited copper layer (∼ 10 μm) using an electrolyte of 75 g/L of $CuSO_4{\cdot}5H_2O$ and 30 g/L of H_2SO_4. This composite conductive layer of gold and copper severed as cathode and a gold bar with a diameter of 2 mm was used as anode. The applied voltage (1.2 V) was applied and the electrolyte was an aqueous solution of $Na_3Au(SO_3)_2$ (75 g/L). All the electrodeposition processes were monitored by a programmed voltage source/picoammeter (6482, Keithley, USA). The morphologies of the samples were examined using scanning electron microscopy (SEM, NanoSEM 450, FEI) after dissolving the PC templates with dichloromethane. To characterize the optical properties with UV-Vis-NIR extinction spectroscopy (Perkin-Elmer, Lambda 900), the cathode layer consisting of sputtered gold and electrodeposited copper of each sample was removed simply by peeling-off and the nanowire arrays remained embedded in the PC template. The plasmonic resonance properties were analyzed by the finite-difference time-domain (FDTD, Lumerical Inc.) method. The dielectric function of gold was interpolated from the materials database (Johnson and Christy). The sizes of mesh were 5 nm × 5 nm × 10 nm.

3. Results and discussion

The basic concept of our fabrication approach relies on the ion-track template method which has been widely adopted to synthesize arrays of parallel aligned nanowires with excellent control over the wire diameter, morphology, crystallinity, axial orientation alignment, and areal density. Generally, nanowires grown in an ion-track template have uniform and identical diameter, which has been recognized as a unique advantage of the method. Such an advantage substantially stems from the uniform etching among ion tracks, or in other words, for different ion tracks the same etching time would produce equal diameter of nanopores. Taking benefit of such an unparallel etching property of ion tracks, in this work, we innovate a new type of ion-track template which contains nanopores with gradient and programmable diameters. This is realized by a proposed experimental protocol where sequential multiple irradiations and track etchings are employed. Figure 1 schematically details the flow chart of the protocol. First, a polycarbonate foil is irradiated with swift heavy ions (25 MeV/u ^{86}Kr in the present work) and the irradiation creates ion tracks in the foil due to the electronic energy loss of the ions. The ion tracks in polymers are known to be damaged regions rich in radicals,

newly formed free volume resulting from degassing of volatile products, and compact resulting from shock waves during the ion impact and cross-linking.[29] For a given material, there exists a threshold of electronic energy loss and above the threshold ion tracks can be etched and ultimately transformed into pores. For polycarbonate it was reported the threshold is 0.25 keV/nm.[30] According to the Monte Carlo simulations using SRIM 2013, the electronic energy loss of the 25 MeV/u ^{86}Kr in polycarbonate is calculated to be 2.8 keV/nm which is more than 10 times of the reported threshold. This guarantees that the Kr ion tracks are etchable and pores with uniform diameter can be obtained. To make a porous template, the Kr ion tracks are etched at 50 °C with an etchant comprising of an aqueous solution of NaOH (5 mol/L in this work). Under such fixed conditions, the pore diameter is solely determined by etching time.[31] The combination of one sequence of irradiation and track etching gives rise to conventional ion track template in which all pores have an identical diameter. Such a porous template has been commonly utilized to electrochemically synthesize high quality nanowires.[32,33] In this work we innovate this conventional ion track template method by introducing multiple sequences of ion irradiation and track etching. Such an innovation endows the method with previously unachievable abilities that gradient and programmable diameters can be realized. To achieve this, multiple sequences of ion irradiation and track etching are adopted, as depicted in Fig. 1(a). After the first etching, the porous template is further irradiated for the second time which is followed by second track etching. The second irradiation produces additional number of ion tracks, depending on the irradiation fluence. The second etching not only transforms the second batch of ion tracks into pores, but also enlarges the diameter of the first batch of pores, and ultimately forming pores with two levels of diameter. It is worth mentioning that the enlargement of the diameter of the first batch of pores is exactly, in principle, the same as the diameter of the second batch of pores. Such a diameter correlation reflects that both diameters are predictable and therefore easily facilitate to meet the demand. When the third sequence is introduced, both of the first and the second batches of diameter are enlarged in a controllable means. Correspondingly in the same way, multiple sequences of irradiation and etching can be further adopted, upon design. Based on these porous templates, nanowires of certain materials can be synthesized by, for example, commonly used electrochemical deposition. Consequently, as demonstrated in Fig. 1(b), arrays with one diameter, two diameters, three diameters, and even more diameters are obtained, relying on the applied sequences. Such nanowire arrays with gradient and programmable diameters represent a previously unachieved level of control in nanowire fabrication and would lead to new physical phenomena of interest, for instance, light management, and a wide spectrum of applications.

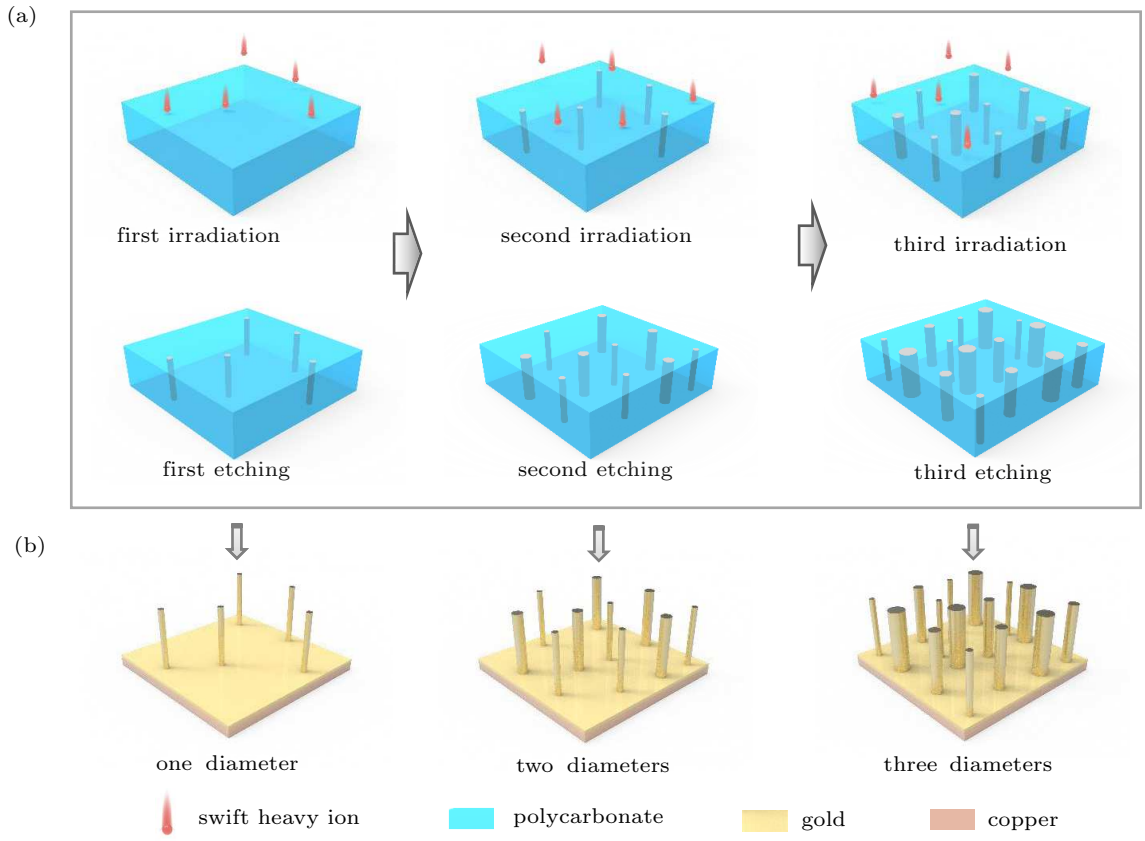


Fig. 1. Schematic illustration of the fabrication procedures of nanowire arrays with gradient and programmable diameters. (a) Template sequential irradiation and track etching and (b) electrochemical deposition of nanowire arrays.

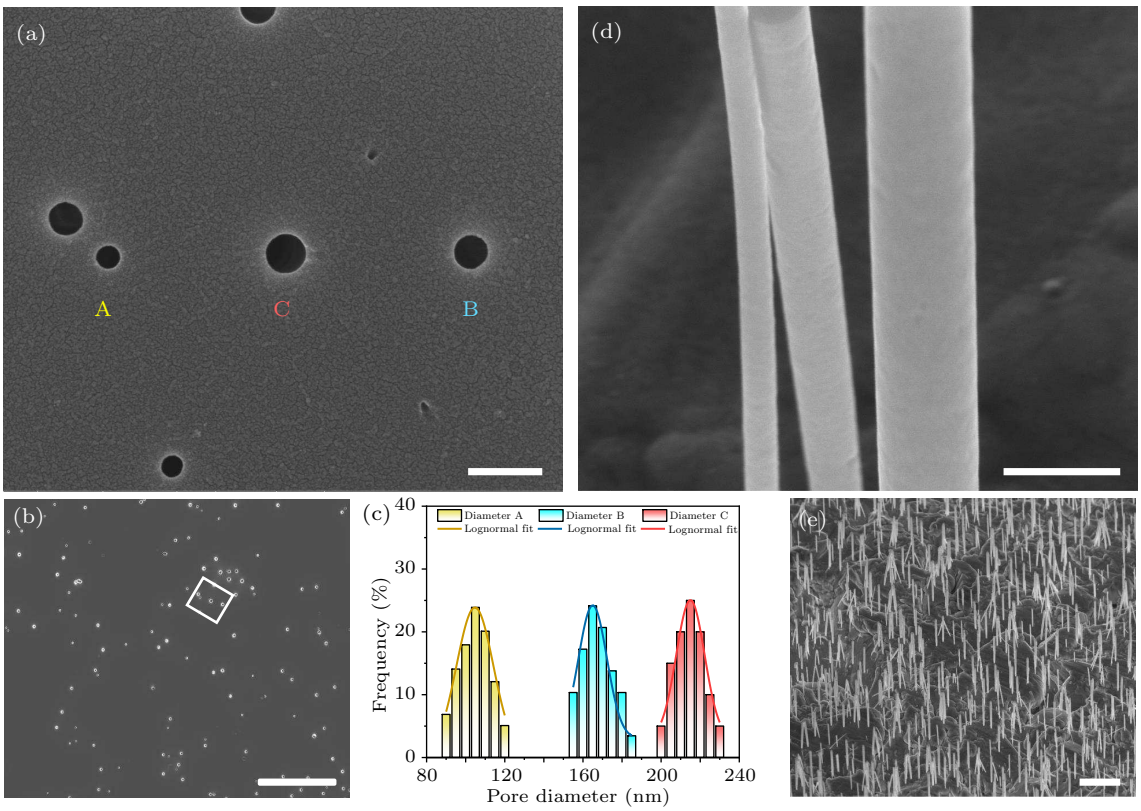


Fig. 2. SEM analyses of as-prepared ion track-etched templates and as-grown gold nanowires with three diameters. (a) Magnified SEM image of a template with three diameters of 105 nm, 165 nm, and 215 nm. (b) Low-magnification SEM image of a template showing random and uniform distribution of nanopores. (c) Statistics on pore diameters disclosing three different diameters. (d) Magnified SEM image of fabricated gold nanowires with three diameters. (e) Low-magnification SEM image of a nanowire array of three diameters. Scale bars are 400 nm (a), (d) and 4 μm (b), (e).

Based on the innovative templates, we have experimentally implemented the fabrication of nanowire arrays with gradient and programmable diameters, using chemically inert gold as a model material. Figure 2 shows SEM images of the representative fabricated ion track templates and grown gold nanowires. Figure 2(a) displays a magnified SEM image of a template containing three diameters, i.e., 105 nm (indicated by A), 165 nm (B), and 215 nm (C). The template was fabricated via three sequences of ion irradiation and etching. It is seen clearly that all pores have perfect circular shape which is believed as the result of the sufficiently high electronic energy loss (2.8 keV/nm) of the swift heavy ions (25 MeV/u ^{86}Kr) and the high homogeneity of the template material (polycarbonate). It should be stressed again that, the respective diameters of nanopores can be well selected, upon demand. The low-magnification SEM image of the template displays that the nanopores are randomly but uniformly distributed at the surface. The random distribution substantially results from the random hits of the incident ions, which is alike to that of rain drops on a flat plane, and both obey the Poisson distribution. The statistics (Fig. 2(c)) on the wire diameter further disclose that there coexist three largely different diameters, namely, 105 ± 15 nm, 170 ± 15 nm, and 215 ± 15 nm, evidencing the success of achieving gradient and programmable diameters enabled by the proposed method of sequential ion irradiation and track etching. Template-assisted electrodeposition has been proven a powerful method for synthesis metallic nanowire arrays with replicated shape and size of pores in a template. We have adopted this method for fabricating gold nanowire arrays within our templates with nanopores of gradient diameters. Figure 2(d) shows an array of nanowires with three diameters, i.e., 120 nm, 210 nm, and 350 nm. One can see that each wire has cylindrical shape and smooth contour, reflecting the superiority of the ion track template method. The SEM image displayed in Fig. 2(e) shows that all wires, despite three diameters, are parallelly aligned and vertically standing on the template. The spatial distribution of the wires is random and uniform, which is identical to the nanopores.

Among diverse nanostructures, nanowires have attracted a great deal of interest because of their unique properties endowed by cylindrical shape. In particular, nontrivial optical properties of metallic nanowires have catalyzed sustained research for pursuing tunable optical responses, including rational light management, and understanding the physics underneath. In this work, we have studied the optical properties of nanowire arrays with gradient and programmable diameters, with peculiar attention on rational light management. Figure 3 shows the optical properties of nanowire arrays with one, two, and three diameters, respectively. In Fig. 3(a), the green curve represents the extinction spectra of a nanowire array with a single diameter of 150 nm, and the blue curve displays the spectra of an array of nanowires with a diameter

of 350 nm. Each spectrum has a main peak, which locates at 750 nm and 1060 nm, respectively. For both arrays, the areal density of nanowires is 1×10^7 cm^{-2}. The red curve manifests the extinction spectrum of an array of nanowires with two diameters which are the same to the two single ones. The peaks' positions are fairly the same to the ones of single diameters. It is believed that the optical response of the gold nanowires stems from surface plasmon resonances which are collective oscillations of the free electron gas inside the structure when they are excited by the incident light. To analyze the resonance mode of the peaks, we have performed full-wave electromagnetic simulations by using the finite-difference time-domain (FDTD) method. In simulations, single wires of each diameter are illuminated at two peak wavelengths by a linearly polarized plane wave, respectively, and the wave-vector is parallel to the wire length. All field profiles displayed in Fig. 3(b) exhibit exotic dipolar resonance despite different excitation wavelengths. Therefore, the optical response of the nanowires is dominated by dipolar plasmon resonance. Also noteworthy is that the field strength is highly dependent on the excitation wavelength. For the thinner wire of 150 nm in diameter, the maximum intensity occurs when the excitation of 750 nm is used whereas the wire of 350 nm in diameter has the maximum field strength when the excitation of 1060 nm is employed. This implies that an array of nanowire with single diameter only has a diameter-dependent resonance peak and limited bandwidth of resonance, which is in good agreement with the experimental observations shown in Fig. 3(a). In contrast, unlike the arrays with single diameters, the array with two diameters exhibits broadband optical response and has two distinct extinction peaks with central wavelengths identical to those of the single diameter nanowires. Such a broadband response should be attributed to successful incorporation of nanowires with two diameters and size-modulated plasmon resonances.[34,35] To confirm this finding, we further combined nanowires of three largely different diameters (100 nm, 170 nm, and 320 nm) into one array, by virtue of the strategy proposed in Fig. 1. As illustrated in Fig. 3(c), from the spectra of the single diameter nanowire arrays, we can see that each single diameter wire array only generates one narrow-band dipolar resonance peak (705 nm, 770 nm, and 970 nm). Very interestingly, a quite broad band response is achieved by integrating three

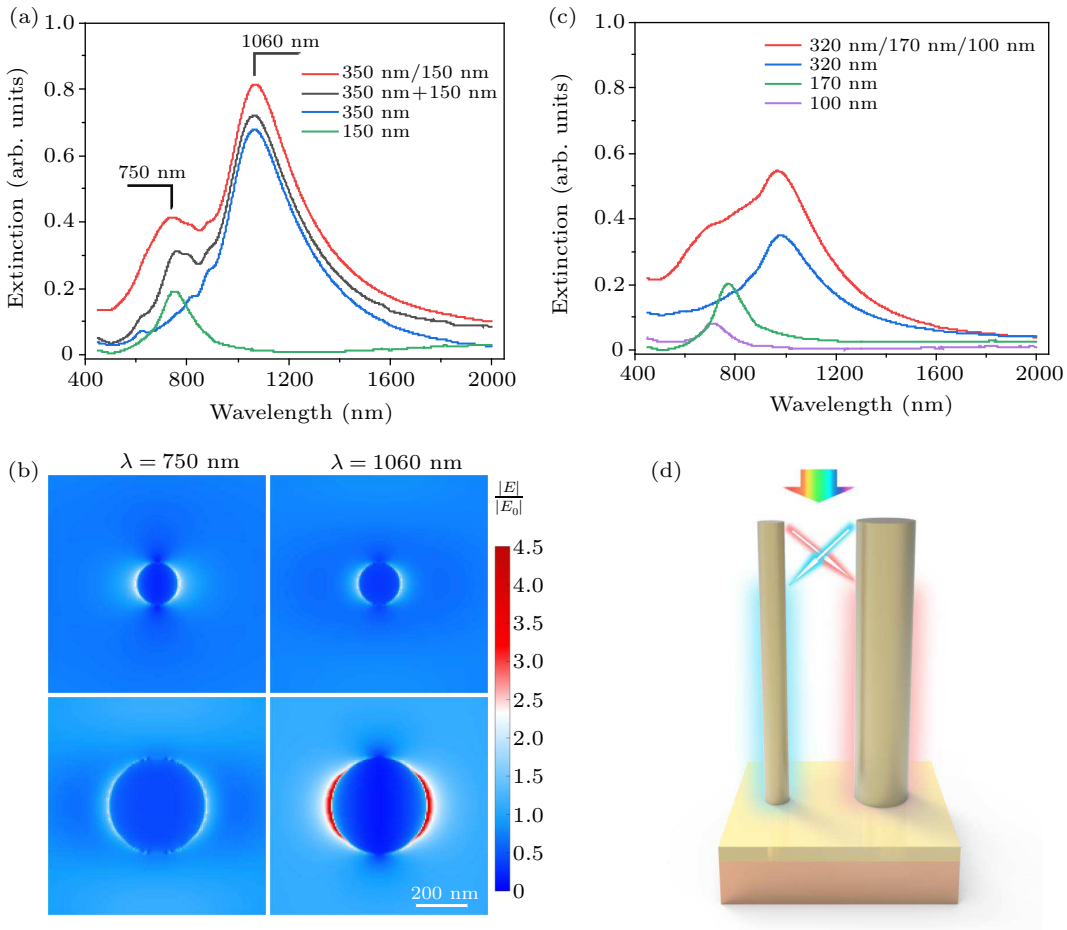


Fig. 3. Optical properties of nanowire arrays with single and multiple diameters. (a) Extinction spectra of arrays of nanowires with single diameters and two diameters. The green curve represents the single diameter of 150 nm and the blue curve displays the array of single diameter of 350 nm. The black curve is the sum of two single diameters. The red corresponds to the spectrum of the array with two diameters (150 nm and 350 nm). (b) Electric field profiles of the nanowires' top. (c) Extinction spectra of arrays of nanowires with single diameters (100 nm, purple; 170 nm, green; 320 nm, blue) and the array with gradient diameters. (d) Schematic illustration of mutual light scattering among nanowires with nonuniform diameters.

dipolar resonances generated by three diameters, which any independent diameter can not. By comparing Figs. 3(a) and 3(c), one should stress here that, in addition to broadband response, band tunability could also straightforwardly implemented by selecting component-nanowire diameters. Based on these observations, one may speculate that even broader band response and tunability could be realized if more diameters were introduced. Additional to broadband response and tunability, enhancing light–matter interaction is another key issue for light management and hence highly desired for many applications such as energy harvesting and conversion, optoelectronic devices. In this work, we have studied the extinction efficiency of nanowire arrays with single diameters and combined diameters. To examine this, we compare the arrays with diameters of 150 nm and 350 nm. The areal density of each is 1×10^7 cm^{-2} and the total is 2×10^7 cm^{-2}. The extinction spectrum is shown as the red curve in Fig. 3(a). On the other hand, the extinction coefficients of two arrays of single diameters are added linearly, according to the Lambert Beer law

$$A = \lg\left(\frac{1}{T}\right) = Kbc,$$

where A is the absorbance (corresponding to extinction in our work), T is the transmittance (transmittance), K, c, and b are the molar absorption coefficient, the concentration of the absorbent, and the thickness of the absorption layer, respectively. By employing this method, the sum is displayed as the black curve in Fig. 3(a). Very inter-diameter interaction is assumed. The enhanced light–matter interaction in arrays of nanowires with gradient diameters is in good agreement with previous theoretical predictions.[19,23–25] The enhancement mechanism could be understood as follows. The gradient diameters can give rise to broadened resonant frequencies which, in turn, lead to enhanced light extinction (scattering and absorption),[21,25,36] as schematically illustrated in Fig. 3(d). In this case, the extinction at the original off-resonance frequency is enhanced by multiple inter-diameters scattering and the original on-resonance maintains almost unchanged. Such a mechanism was further investigated with a mode-based numerical method in combination with an analytic approximation and it was found that diameter nonuniformity can indeed enhance absorption and, in consequence, the ultimate photovoltaic efficiency of silicon nanowire arrays.[26,37]

4. Conclusion

In summary, we have proposed and experimentally demonstrated a new fabrication strategy for creating nanowire arrays with gradient and programmable diameters towards rational light management. The core of the strategy is the innovation of sequential ion irradiation to create ion tracks in polymer foils and ion track etching, relying on high flexibilities of the ion track technology. Taking benefit of this strategy, we have fabricated gold nanowire arrays with two and three diameters respectively. Optical characterizations show that broadband, tunable, and enhanced plasmonic responses can be achieved using the nanowire arrays with gradient diameters. We expect that the fabrication strategy of sequential ion irradiation and track etching would be readily extended to fabricating complex nanostructures which could find great potential in applications such as light management, enhanced spectroscopies, and optoelectronic devices.

Acknowledgment

The authors thank the HIRFL operation team for preparing $^{86}Kr^{26+}$ SHI beams.

References

[1] Leung S F, Zhang Q, Xiu F, Yu D, Ho J C, Li D and Fan Z 2014 *J. Phys. Chem. Lett.* **5** 1479
[2] Wang W and Qi L 2019 *Adv. Funct. Mater.* **29** 1807275
[3] Villa K, Novotný F, Zelenka J, Browne M P, Ruml T and Pumera M 2019 *ACS Nano* **13** 8135
[4] Wang J, Xiong Z, Zhan X, Dai B, Zheng J, Liu J and Tang J 2017 *Adv. Mater.* **29** 1701451
[5] Gong X, Tong M, Xia Y, Cai W, Moon J S, Cao Y, Yu G, Shieh C L, Nilsson B and Heeger A J 2009 *Science* **325** 1665
[6] Han J, Yang D, Ma D, Qiao W and Wang Z Y 2018 *Adv. Opt. Mater.* **6** 1800038
[7] Zhong Z, Li X, Wu J, Li C, Xie R B, Yuan X, Niu X, Wang W, Luo X, Zhang G, Wang Z M, Tan H H and Jagadish C 2019 *Appl. Phys. Lett.* **115** 053101
[8] Garin M, Heinonen J, Werner L, Pasanen T P, Vahanissi V, Haarahiltunen A, Juntunen M A and Savin H 2020 *Phys. Rev. Lett.* **125** 117702
[9] Wang Y, Li H, You L X, Lv C L, Wang H Q, Zhang X Y, Zhang W J, Zhou H, Zhang L, Yang X Y and Wang Z 2019 *Chin. Phys. B* **28** 078502
[10] Guo D, Li W, Wang D, Meng B, Fang D and Wei Z 2020 *Chin. Phys. B* **29** 098504
[11] Li W, An Y, Wienk M M and Janssen R A J 2015 *J. Mater. Chem. A* **3** 6756
[12] Negash A, Genene Z, Thiruvallur Eachambadi R, Kesters J, Van den Brande N, D'Haen J, Penxten H, Abdulahi B A, Wang E, Vandewal K, Maes W, Mammo W, Manca J and Admassie S 2019 *J. Mater. Chem. C* **7** 3375
[13] Rodrigo D, Limaj O, Janner D, Etezadi D, Garcia de Abajo J, Pruneri V and Altug H 2015 *Science* **349** 165
[14] Fu X, Ren F F, Sun S, Tian Y, Wu Y, Lou P and Du Q G 2019 *Phys. Scripta* **94** 055504
[15] Jaiswal R, Bharambe J, Patel N, Dashora A, Kothari D C and Miotello A 2015 *Appl. Catal. B Environ.* **168** 333
[16] Momeni M M, Ghayeb Y and Gheibee S 2017 *Ceram. Int.* **43** 564
[17] Feng K, Wang S, Zhang D, Wang L, Yu Y, Feng K, Li Z, Zhu Z, Li C, Cai M, Wu Z, Kong N, Yan B, Zhong J, Zhang X, Ozin G A and He L 2020 *Adv. Mater.* **32** 2000014
[18] Zheng J, Wang J, Xiong Z, Wan Z, Zhan X, Yang S, Chen J, Dai J and Tang J 2019 *Adv. Funct. Mater.* **29** 1901768
[19] Liu C, Zhang H, Sun Z, Ding K, Mao J, Shao Z and Jie J 2016 *J. Mater. Chem. C* **4** 5648
[20] Shang Q, Li C, Zhang S, Liang Y, Liu Z, Liu X and Zhang Q 2020 *Nano Lett.* **20** 1023
[21] Yu P, Wu J, Liu S, Xiong J, Jagadish C and Wang Z M 2016 *Nano Today* **11** 704
[22] Cao L, White J S, Park J S, Schuller J A, Clemens B M and Brongersma M L 2009 *Nat. Mater.* **8** 643

[23] Cao L, Fan P, Vasudev A P, White J S, Yu Z, Cai W, Schuller J A, Fan S and Brongersma M L 2010 *Nano Lett.* **10** 439
[24] Zheng J, Dai B, Wang J, Xiong Z, Yang Y, Liu J, Zhan X, Wan Z and Tang J 2017 *Nat. Commun.* **8** 1438
[25] Bao H and Ruan X 2010 *Opt. Lett.* **35** 3378
[26] Sturmberg B C P, Dossou K B, Botten L C, Asatryan A A, Poulton C G, McPhedran R C and Martijn de Sterke C 2012 *Appl. Phys. Lett.* **101** 173902
[27] Hong L, Rusli, Wang X, Zheng H, Wang H and Yu H 2014 *J. Appl. Phys.* **116** 194302
[28] Lin C and Povinelli M 2011 *Opt. Express* **19** A1148
[29] Fink D 2004 *Transport Processes in Ion-Irradiated Polymers*, 1st edn. (New York: Springer-Verlag) pp. 171–200
[30] Fleischer R L, Price P B and Walker R M 1975 *Nuclear Tracks in Solids: Principles and Applications*, 1st edn. (California: Berkeley) p. 20
[31] Duan J L, Liu J, Yao H J, Mo D, Hou M D, Sun Y M, Chen Y F and Zhang L 2008 *Mater. Sci. Eng. B* **147** 57
[32] Liu J, Duan J L, Toimil-Molares M E, Karim S, Cornelius T W, Dobrev D, Yao H J, Sun Y M, Hou M D, Mo D, Wang Z G and Neumann R 2006 *Nanotechnology* **17** 1922
[33] Toimil-Molares M E 2012 *Beilstein J. Nanotechnol.* **3** 860
[34] Giannini V, Fernandez-Dominguez A I, Heck S C and Maier S A 2011 *Chem. Rev.* **111** 3888
[35] Wen L, Xu R, Mi Y and Lei Y 2017 *Nat. Nanotechnol.* **12** 244
[36] Fountaine K T, Kendall C G and Atwater H A 2014 *Opt. Express* **22** A930
[37] Du Q G, Kam C H, Demir H V, Yu H Y and Sun X W 2011 *Opt. Lett.* **36** 1884